Materials Science & Engineering C 112 (2020) 110968

Contents lists available at ScienceDirect

Materials Science & Engineering C

journal homepage: www.elsevier.com/locate/msec

Antibacterial composite hybrid coatings of veterinary medical implants

Magdalena Ziąbka[a,*], Joanna Kiszka[b], Anita Trenczek-Zając[c], Marta Radecka[c], Katarzyna Cholewa-Kowalska[d], Igor Bissenik[e], Agnieszka Kyzioł[f], Michał Dziadek[d,f], Wiktor Niemiec[g], Aleksandra Królicka[h]

[a] Department of Ceramics and Refractories, Faculty of Materials Science and Ceramics, AGH University of Science and Technology, Krakow 30-059, Poland
[b] Faculty of Electrical Engineering, Automatics, Computer Science and Biomedical Engineering, AGH University of Science and Technology, Krakow 30-059, Poland
[c] Department of Inorganic Chemistry, Faculty of Materials Science and Ceramics, AGH University of Science and Technology, Krakow 30-059, Poland
[d] Department of Glass Technology and Amorphous Coatings, Faculty of Materials Science and Ceramics, AGH University of Science and Technology, 30-059 Krakow, Poland
[e] Veterinary Clinic "Pulawska", 02-844 Warsaw, Poland
[f] Faculty of Chemistry, Jagiellonian University, 30-387 Krakow, Poland
[g] Department of Silicates and Macromolecular Compounds, Faculty of Materials Science and Ceramics, AGH University of Science and Technology, Krakow 30-059, Poland
[h] University of Gdansk, Intercollegiate Faculty of Biotechnology UG-MUG, Laboratory of Biologically Active Compounds, Gdansk 80-307, Poland

ARTICLE INFO

Keywords:
Metallic implants
Silver nanoparticles
Composite hybrid layers
Physicochemical and biological properties

ABSTRACT

The aim of the work was to develop innovative antibacterial hybrid coatings applied on implants that are used for anastomoses of animals' long bones and to assess their physicochemical and biological properties. Plates made of the titanium alloy were covered with composite hybrid layers so as to protect the implant surface against corrosion and to enhance it with antibacterial properties.The hybrid coatings were obtained electrochemical oxidation and sol-gel. First, a layer of titanium nanotubes was applied to the implants surface through anodization. Next, the sol-gel method was used to create the second layer with silver nanoparticles. The microstructure examination of the materials was performed with the SEM. The phase composition analysis was carried out via the X-ray diffraction. The surface parameters (roughness, contact angle and free surface energy) were assessed. Biological studies of implants were conducted, including the analysis of degradation processes, cell response and bactericidal activity. The results confirmed that the hybrid antibacterial layers effectively protected the implant surface against scratches and corrosion and eliminated bacteria, which in turn would promote bone healing. The advantageous physicochemical and biological properties of metallic implants with hybrid composite layers raise hopes for their applicability in the veterinary treatment of bone fractures.

1. Introduction

The development of medicine and implantology makes prostheses and implants a popular solution to treat not only humans but also animals. Nowadays, it is a common view point that animals require medical help and treatment just as people do, particularly as numerous fractures of limbs result from the inappropriate diet, genetic defects or vehicular accidents.

The aim of any fracture treatment is to fully restore the limb functionality as quickly as possible. The stable realignment of bones and the full restoration of the joint motionare necessary for the complete limb functionality. Osteosynthesis attempts to achieve this goal in a minimally invasive fashion, using implants for internal or external fixation [1]. It is becoming more and more popular to adapt internal fixation techniques used for humans to treat animals as well. There are well-known implants used in veterinary medicine, such as: Steinmann pins, Kirschner wires, Rush pins, Kuntscher nails, bone wires, locking plates and external fixators [2]. The fracture treatment depends mainly on the type of injury and the animal age [3].Open fractures,where the risk of infection is high, are treated in a manner different from closed fractures. Veterinary devices and implants for osteosynthesis come in various shapes, e.g. nails, wires, screws and plates. Screws and plates are applied to treat diaphyseal and comminuted fractures of long bones, including fractures into joints. There is also a variety of implants

* Corresponding author.
E-mail addresses: ziabka@agh.edu.pl (M. Ziąbka), anita.trenczek-zajac@agh.edu.pl (A. Trenczek-Zając), radecka@agh.edu.pl (M. Radecka), cholewa@agh.edu.pl (K. Cholewa-Kowalska), kyziol@chemia.uj.edu.pl (A. Kyzioł), dziadek@agh.edu.pl (M. Dziadek), wniemiec@agh.edu.pl (W. Niemiec), aleksandra.krolicka@biotech.ug.edu.pl (A. Królicka).

https://doi.org/10.1016/j.msec.2020.110968
Received 19 March 2020; Received in revised form 11 April 2020; Accepted 12 April 2020
Available online 14 April 2020

materials, such as metal and metal alloys (stainless steel, titanium, titanium alloys), ceramics or biodegradable and nondegradable polymers. The choice of implant material depends on the anatomical location and expected functions of the device [4]. In general, metals possess the best mechanical properties - they are strong, stiff and ductile. Therefore, metal implants are highly recommended for animals whose activeness results in high load transfer through bones. Titanium-based metals are widely used for load-bearing orthopedic applications, thanks to their excellent mechanical properties and good biocompatibility [5,6]. Unfortunately, there are common cases of infections caused mainly by *Staphylococcus aureus* and *Escherichia coli* bacteria that lead to the implant failures. In order to prevent infections it seems essential to endow metallic implants with antibacterial properties [7,8]. Recent studies have proven that surface modifications are an effective strategy to achieve this goal [9–11]. Another popular biomaterial used for internal fixation devices is stainless steel that has been used for decadesas an implantable material [12] thanks to its advantageous combination of mechanical properties, corrosion resistance and cost effectiveness, in comparison to other metallic implant materials.

The majority of internal fixation surgeries properly restore functionality of the fractured bones. The successful fracture treatment consists in: selecting an appropriate implant, immobilizing the fracture site, preserving blood supply and eliminating the risk of infection. Open fractures are much more prone to infections that might lead to the implant removal and re-operation. One of the main challenges for the implant design is to improve the bone-to-implant connection. Osteointegeration, which is the direct connection of bone and implant, involves chemical bonding as well as micro- and macro-level mechanical interlocking of the bone tissue with the implant surface. Chemical and morphological modifications of the implant outer surface might enhance the connection strength and reduce the healing time. So far, bioactive ceramics, e.g. hydroxyapatite, tricalcium phosphate and bioglasses, have been used as coatings on the implant surface. Such coatings improve the bone-implant connection through chemical bonding. The surface morphology of implants can be modified with external threads, undercuts and layers of wires on the macrolevel and by increasing the surface roughness in the microscale [13]. Obtaining the antibacterial function of implants is even more important than their bioactivity. The degree of bone infection is influenced by the type and virulence of the micro-organisms present at the bone damage site. Sometimes the infection can be subdued with antibiotics, yet severe cases of inflammation do occur, which might lead to bone necrosis [14]. Therefore, the antibacterial effectiveness against bacteria, such as Gram-positive *Staphylococcus aureus* and Gram-negative *Escherichia coli*, is an important issue. What is more, it is necessary to develop new methods of dealing with chronic infections due to the increasing antimicrobial resistance. The antibacterial characteristics of implants can be enhanced through mechanical, physical, chemical and biochemical surface modifications. Recently the electrochemical anodization has been recognized as a cost-effective, versatile and simple method of the surface modification that provides medical implants with highly ordered nanotubular titanium oxide (TiO_2) layers [15,16]. Such layers facilitate osteointegration through more efficient bone cell adhesion, differentiation, ALP activity, bone matrix deposition, apatite deposition rates [17], and hemocompatibility of Ti and Ti-based materials [18–20].

Hybrid antimicrobial nanolayers prepared through the sol-gel method ensure the local release of silver, copper and zinc cations on the surface endowed with high bactericidal activity. The conventional sol-gel methods for obtaining tightly adhering oxide nanolayers require relatively high temperatures (around 500 °C) and thus they are problematic for medical institutions. On the other hand, organic-inorganic hybrid nanolayers based on 3-(trialkoxysilyl) propylmethacrylate and glicydoxy-propyl-trialkoxysilane, titanium izopropoxide/zirconium izopropoxide formed with interconnected polymer 3D silica networks (partially substituted by titanium atoms instead of silicon atoms) and polymethyl methacrylate networks containing silver, copper and zinc cations (ionically bonded to silica) prepared by the sol-gel method are very promising for medical applications [21,22]. Nanolayers without bonded heavy metal cations can be potentially applied for other purposes as well, e.g. as organic immobilization agents (drugs, enzymes etc.) or as inert or conversely active interlayers in biomedical applications [23].

Properly designed materials might offer various post-surgical reactions. Taking into consideration requirements established for implants, an ideal material should be biocompatible and resistant to corrosion. It should also be endowed with certain biological and mechanical properties confirmed by thorough examinations.

To summarize, modern implants should not only facilitate the tissue regeneration and accelerate the implant-bone integration but also prevent inflammation caused by microorganisms. The materials surface modifications, e.g. addition of bioactive, biostatic and bactericidal agents may help to achieve this goal. The aim of this work was to develop antibacterial composite hybrid layers of medical devices used for osteosynthesis of animal bone fractures. The proposed layers were to protect implants against scratches and microbial corrosion, and to improve cell adhesion by means of bactericidal modifications.

In this work we applied composite hybrid layers in a processes of anodization and sol-gel on the veterinary implants and performed the complex evaluation of their physicochemical and biological properties. To study the microstructure and chemical composition of layers we engaged the scanning electron microscopy equipped with energy dispersive spectrometer and X-Ray diffraction. We also used the AFM, profilometry and the sessile drop method to investigate the surface properties.The biological properties in the in vitro environment were evalueated in order to prove antibacterial efficacy against Gram-positive and Gram- negative bacteria and cell viability of human osteoblastic and keratinocytes cells. Such parameters as cells adhesion, proliferation, percentage of live, early apoptotic, late apoptotic and dead human osteoblastic cells were investigated. To evaluate the layers stability in the in vitro conditions the ICP-MS spectrometric analysis was performed. We checked the concentration of metal ions in the culture media and distilled water.

2. Results and discussion

According to the examination results, the surface microstructure of the implants on theTi-6Al-4V titanium alloy matrix coated with the TiO_2 nanotubes layer and the hAg hybrid coating with bactericidal properties is smooth, with only small scratches resulting from the surface treatment process (Fig. 1A). Basing on the EDX chemical analysis, the percentage chemical composition of the TiAlV alloy was determined at the point marked in the photo as follows: titanium 85%, aluminum 7% and vanadium 8%. In Fig. 1B, the TiO_2 nanotubes layer obtained through the anodization is visible. The observations have revealed that the nanotubes layer is continuous and it covers the implants surface evenly. The layer thickness is in the range of 550-600 nm. The manufactured nano structures are morphologically homogeneous and their diameters range from 50 nm to 60 nm. The EDX analysis confirmed the TiO_2 presence on the implants surface, which was also revealed in the XRD studies. The chemical composition determined at the point was: titanium 72%, aluminum 5%, vanadium 6% and oxygen 17%. The SEM observations conducted for the TiAlV/TiO_2/hAg plate (Fig. 1C) have confirmed that the hybrid layer completely covers the TiO_2 nanotubes layer. The layer is continuous and on its surface there are evenly distributed silver nanoparticles resulting from the thermochemical reduction process (particle size is 20-35 nm on average). The EDX analysis also confirmed the presence of silver in the outer hybrid coating. The chemical composition at the point is: titanium 44%, aluminum 3%, vanadium 3%, oxygen 21%, silver 20%, carbon 5% and silicon 4%.

The microstructural analysis of the implants proved the perfect coverage of the elements obtained via the electrochemical oxidation

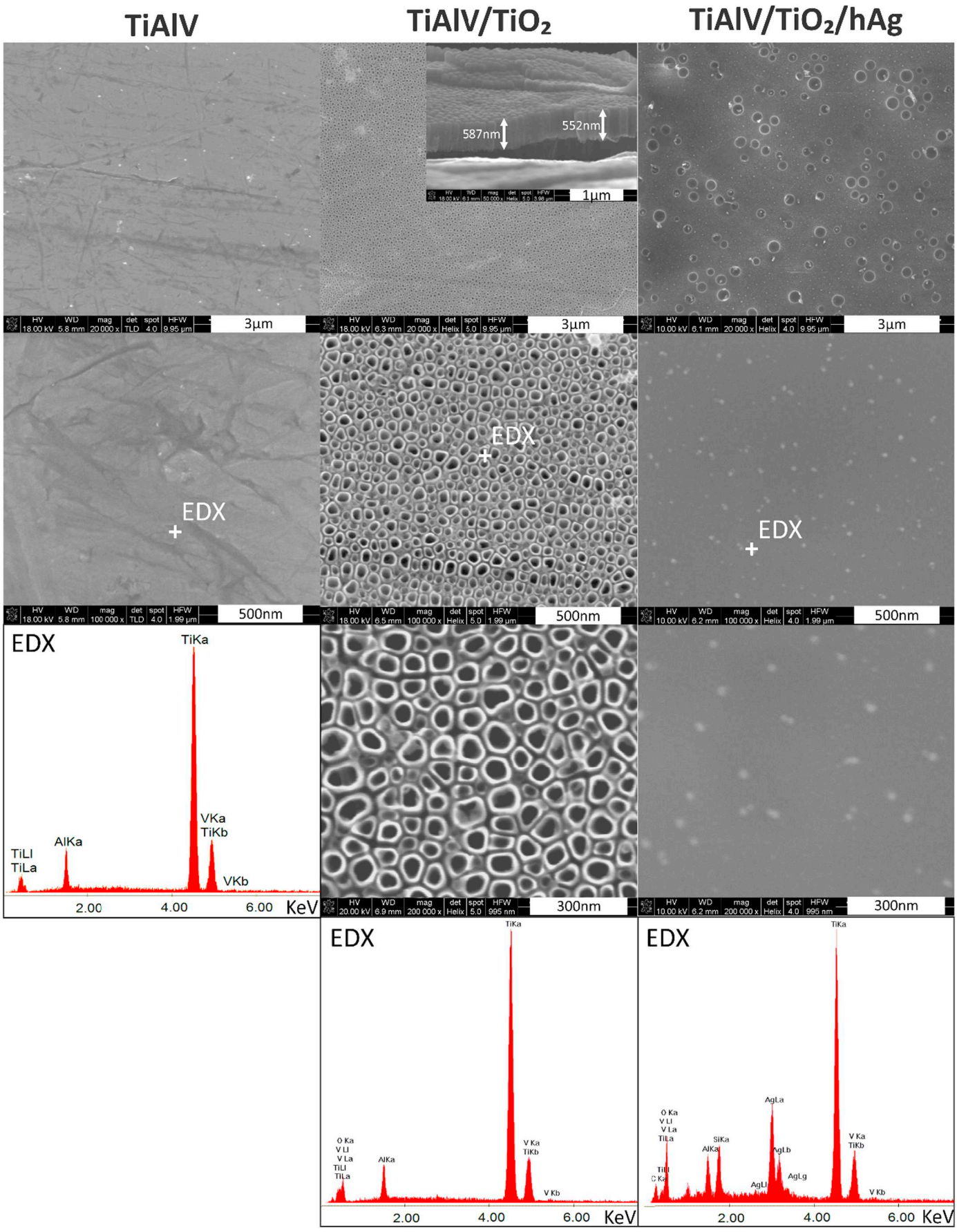

Fig. 1. SEM images and EDX spectra of titanium alloy (TiAlV), TiO_2 nanotubes layer on titanium alloy (TiAlV/TiO_2), and sol-gel layer with silver nanoparticles on TiO_2 nanotubes layer (TiAlV/TiO_2/hAg).

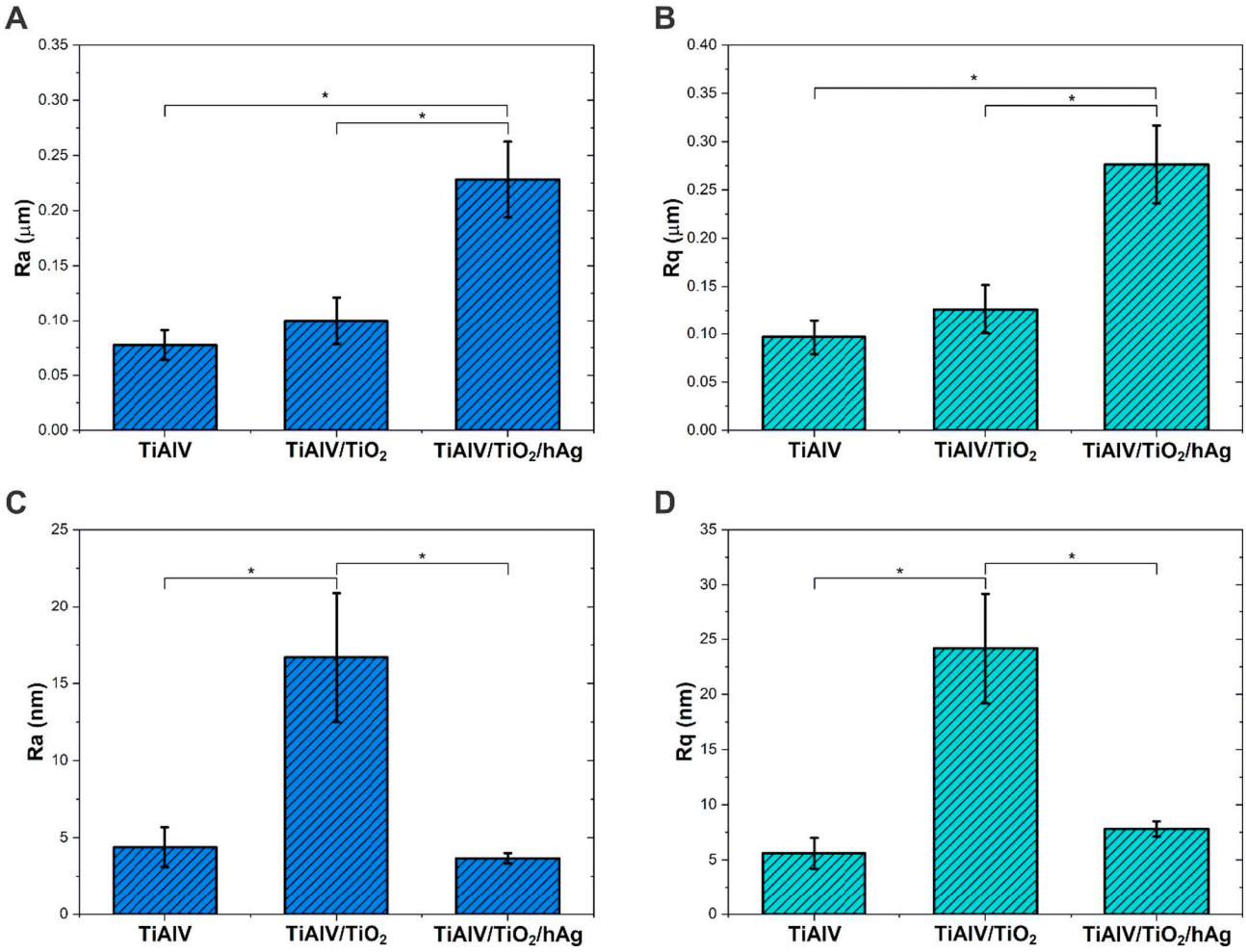

Fig. 2. Surface roughness parameters; *Ra* (A) and *Rq* (B) of investigated samples measured with contact profilometer; *Ra* (C) and *Rq* (D) of investigated samples measured with AFM. Statistically significant differences ($p < 0.05$) are indicated by asterisks.

and the sol-gel methods, even in the case of such complex shapes as bone anastomosis plates. The literature data confirm that the TiO_2 nanotubes layer promotes bone cells functionality in vitro and bone-implant osseointegration in vivo [24,25]. Moreover, due to the hollow-core structure, the titanium oxide nanotubes are known to be a drug loading and delivery platform for bactericidal elements, e.g. silver, which provides a relatively long-term antibacterial activity and the good tissue-implant integration [26].

To characterize the topography of metallic materials with applied layers, the surface roughness measurements of the samples were taken with the contact profilometer. The obtained values of *Ra* and *Rq* parameters are presented in Fig. 2A–B. The Ra parameter (determining the arithmetic mean profile deviations from the mean) for both the Ti-6Al-4V titanium alloy and the same material with the TiO_2 nanotube layer do not exceed 0.08 μm and 0.10 μm, respectively. These results prove that the tested materials have a smooth surface. However, the average *Ra* value (approx. 0.23 μm) increased almost three times for the TiAlV/TiO_2/hAg samples, as compared to the initial sample. The *Rq* parameter (the mean square deviation of the roughness profile) is analogous to the Ra parameter. For the TiAlV and TiAlV/TiO_2 samples, the average *Rq* values are similar and do not exceed 0.10 μm and 0.13 μm, respectively. The average *Rq* value increased almost three times for the sample with two layers produced on the Ti-6Al-4V titanium alloy in comparison to the unmodified sample coating.

The silver nanoparticles aggregates present at the points where the profilometer needle touched the TiAlV/TiO_2/hAg material might explain the roughness increase of its surface layer.

The atomic force microscopy method was used to determine the surface nanotopography of the metallic implants and the ones modified with hybrid layers. The slight differences in profile heights seen in the photo for the TiAlV sample were the result of a technological process. The average arithmetic mean roughness (*Ra*) for the first tested sample was 4.4 nm.

The analysis of the TiO_2 nanotubes samples revealed that the nanostructures on the surface of the Ti-6Al-4V alloy resulted in much higher roughness values of the outer surface. The average *Ra* value for the TiAlV/TiO_2 sample increased almost four times in comparison to the TiAlV material and equalled 16.7 nm. The uneven areas are associated with the nanostructure surface and the presence of holes throughout the entire scanned area. The large depressions resulted in the significantly different *Ra* and *Rq* values which are shown in Fig. 2C–D.

In the pictures (Fig. 3) there are no traces of scratches created during the implants production, which means that the TiO_2 nanotubes layer covered all scratches and discontinuities of the Ti-6Al-4V titanium alloy.

The substrate roughness of the TiAlV/TiO_2/hAg sample is definitely lower than of the TiAlV/TiO_2 sample and it has a much smaller value spread. The bigger differences in the *Ra* and *Rq* parameters result from few high elevations that may result from the silver nanoparticle agglomerates formed close to the sample surface. In addition, in the TiAlV/TiO_2/hAg sample the antibacterial coating completely covers the previous layer, which proves the successful layering process obtained via the sol-gel method.

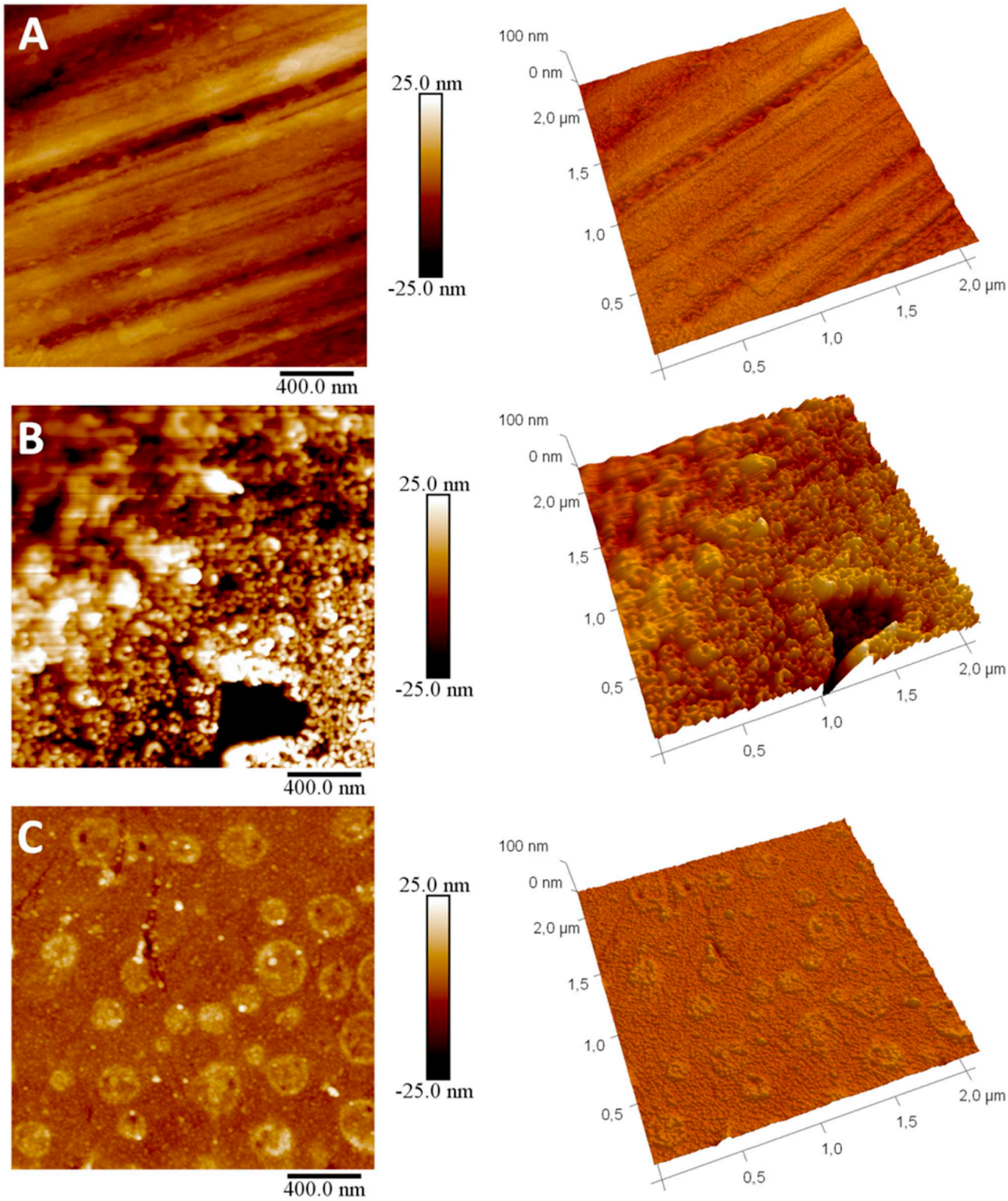

Fig. 3. AFM microscope images of the surface layer of TiAlV (A), TiAlV/TiO_2 (B) and TiAlV/TiO_2/hAg (C) samples.

Considering the applicability of the hybrid materials as medical implants, the increased roughness value may cause both positive and negative phenomena at the implant-tissue interface. The advantage will be the enhanced bone-implant osseointegration. On one hand, micro-topography establishes a strong long-lasting connection between the implant surface and peri-implant bone, leading to the stable mechanical fixation of the implant [27]. On the other hand, nanotopography can promote the attachment of bone cells by enhancing protein adsorption and increasing the contact area with protein and cells. Furthermore, surface nanostructures promote proliferation and differentiation of osteoblastic and mesenchymal cell, ensuring the proper implant-tissue interface. However, there is a risk that the rough surface will attract not only the beneficial osteogenic cells promoting the bone regeneration process, but also microorganisms forming a biofilm which causes inflammation at the implantation site [28]. Still, the introduction of silver nanoparticles would prevent bacterial activity, which was confirmed in

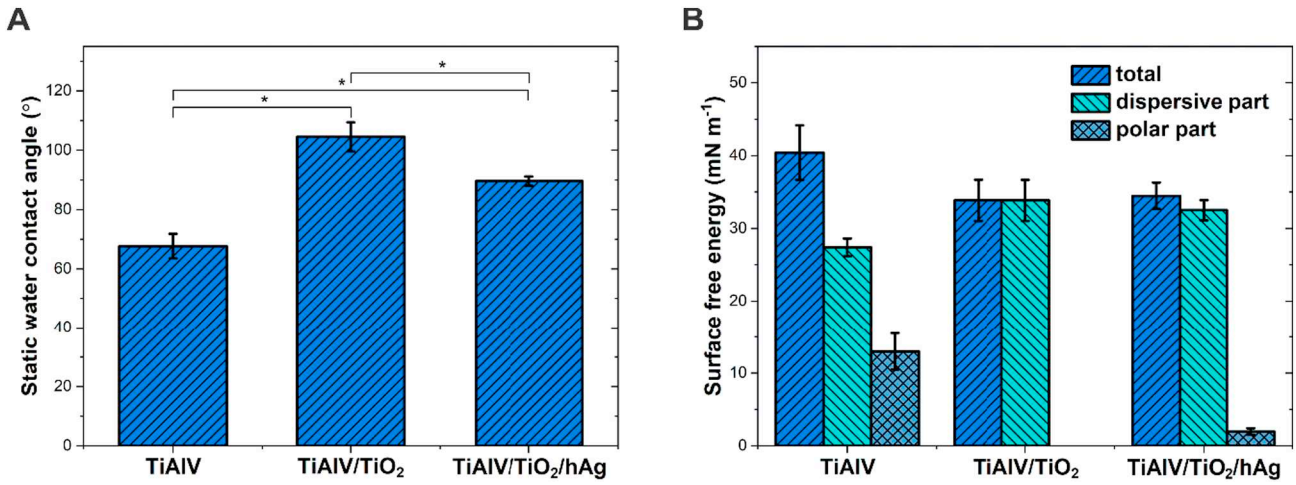

Fig. 4. Static water contact angle (A) and surface free energy (B) of the materials. Statistically significant differences ($p < 0.05$) are indicated by asterisks.

the tests. The modification of nano- and microscale roughness also influences other physicochemical properties, e.g. the higher the roughness, the higher the local surface electrostatic charge density and adhesion energy [29].

The contact angle studies have revealed that the samples from titanium-based alloys have a hydrophilic surface, i.e. they are well wetted by distilled water. The average contact angle values for the TiAlV samples do not exceed 68° and coincide with the literature data [30]. The modification of the substrate with the TiO_2 nanotubes layer via anodization (TiAlV/TiO_2) contributed to the change of the surface character from hydrophilic to hydrophobic, which is confirmed by the obtained contact angle values in the range from 100 to 108°. The sol-gel coating is characterized by significantly lower contact angle values as compared to the values obtained for the sample covered only with the TiO_2 nanotubes layer. The range of θ angle values for the TiAlV/TiO_2/hAg sample is 88–92°. The collective summary of the average contact angle values with a standard deviation is shown in Fig. 4A.

Our results confirmed that the titanium oxide nanotubes formed on the surface of the Ti-6Al-4V titanium alloy facilitate the development of the surface layer at the nanoscale when compared to the sample without coatings. This phenomenon is proved by the contact angle increase by almost 40° and the change in the substrate wettability from hydrophilic to hydrophobic. The second layer providing bactericidal properties for the implants is characterized by a smaller contact angle value than the substrate with the TiO_2 nanotubes layer, yet it is larger than the contact angle of the unmodified TiAlV alloy. The contact angle may increase due to significantly higher microscale surface roughness for the TiAlV/TiO_2/hAg sample. It is well known that the changes in both nano- and microtopography influence surface wettability. However, another crucial factor affecting wettability is the chemical composition of the surface. In the hybrid layer of the TiAlV/TiO_2/hAg sample there are non-polar methyl groups (-CH_3) which may cause an increase in hydrophobicity, as compared to the pure titanium alloy. In turn, the contact angle of the material coated with TiO_2 nanotubes most likely decreases due to the surface development. The lower the contact angle of materials, the higher the free surface energy. This relationship is confirmed by the total free energy tested for the TiAlV sample (Fig. 4B) which has the highest value of all the tested materials (40mN/m ± 4). For the TiAlV/TiO_2 and TiAlV/TiO_2/hAg samples, the total surface energy values decreased by 7mN/m ± 4 and 8mN/m ± 4, respectively, when compared to the Ti-6Al-4V titanium alloy sample. The analysis of the surface energy components (polar and dispersion) showed that for the TiAlV/TiO_2 sample, the total surface energy equals the dispersion component and the value of the polar component is 0mN/m ± 4. Also for the TiAlV/TiO_2/hAg sample the dispersion component value exceeds the polar one. The polar component may be associated with the hybrid layer of OH groups most likely connected to Si (Si-OH) which is present on the surface. In addition, the polar component might be affected by the Ag nanoparticles layer. The polar component of the multilayer system correlates with the slightly lower contact angle of the antibacterial layer in comparison with the nanotubes layer. On the other hand, in the case of the unmodified sample the differences between the dispersion and polar components are significantly smaller - 27mN/m ± 4 and 13mN/m ± 4, respectively.

The surface phase composition analysis of all the samples (TiAlV, TiAlV/TiO_2, TiAlV/TiO_2/hAg) was performed via the X-ray diffraction and the results are shown in Fig. 5. The diffractogram indicates the characteristic peaks originating from the titanium alloy with aluminum and the titanium alloy with vanadium. Titanium is the main component of the Ti-6Al-4V alloy, so the intensity of the peaks originating from the dominant phase is the highest. The TiAlV sample revealed no peaks derived from TiO_2, which might result from the presence of the nanotubes layer on the titanium alloy substrate. After the anodization process, no peaks from the TiV phase (peak around 39° and 57°) are observed and an additional peak of approximately 58° appears on both diffractograms. The SEM microscope images of the TiAlV/TiO_2 samples with the visible TiO_2 nanostructures layer also confirm the successful anodization process.

The phase composition of the plate coated with TiO_2 nanotubes and

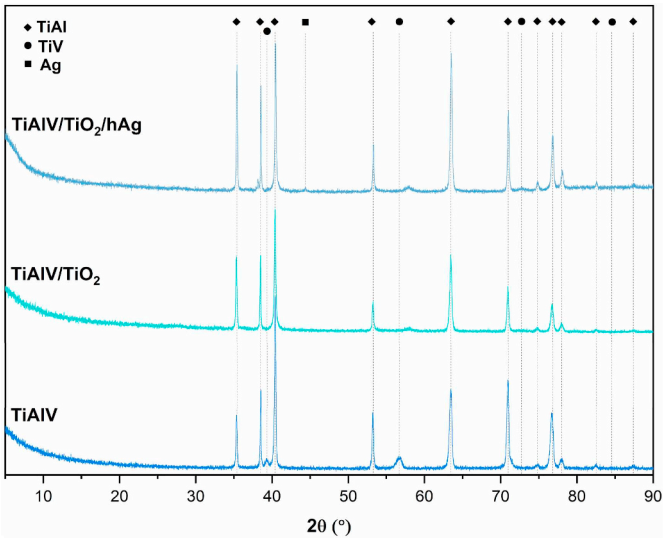

Fig. 5. X-ray diffraction pattern showing the phase composition of the surface layer of the TiAlV, TiAlV/TiO_2 and TiAlV/TiO_2/hAg samples.

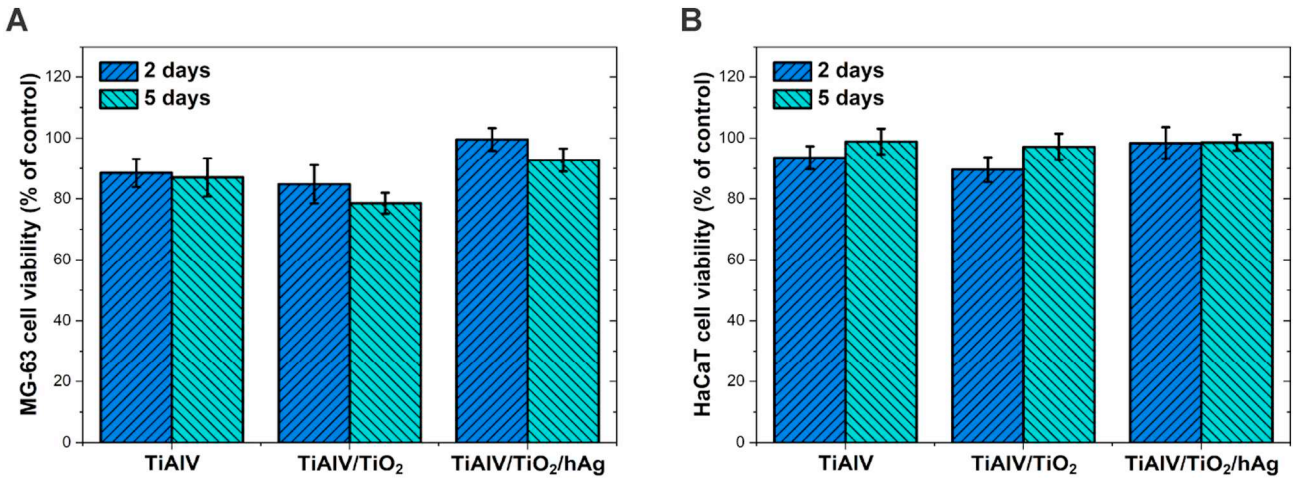

Fig. 6. Cell viability of human osteoblastic cells of the MG-63 (A) line and human keratinocytes of the HaCaT (B) line in direct contact with TiAlV, TiAlV/TiO_2 and TiAlV/TiO_2/hAg samples after two and five days of culture. The results are presented as mean values ± standard deviation. There were no statistically significant differences.

the hybrid antibacterial coating revealed the peaks from the titanium alloy and a distinct small and sharp peak at about 37.5° derived from silver. Therefore, the analysis of the phase composition of the TiAlV/TiO_2/hAg material confirms the presence of silver nanoparticles in the external hybrid coating produced by the sol-gel method.

The influence of the tested alloys on cell viability was assessed during their incubation with two selected cell lines. Fig. 6 shows the survival of MG-63 and HaCaT cell lines after two and five days of the culture. The viability is expressed as a percentage of live cells adhered to the surface of a polystyrene culture plate (a control) in relation to the number of live cells on the unmodified alloy (TiAlV) and the modified alloys ((TiAlV)/TiO_2 and TiAlV/TiO_2/hAg).

The conducted experiment did not show the cytotoxic effect of the modified TiAlV/TiO_2 and TiAlV/TiO_2/hAg alloys. The cells viability results prove that the TiAlV/TiO_2/hAg sample has the lowest cytotoxicity towards the MG-63 cell line after two days of culture, yet the results were not statistically significant. For this material the average percentage of dead cells do not exceed 1% after 2 days of culture and 8% after 5 days. In contrast, the highest cytotoxicity was demonstrated by the sample with TiO_2 nanotubes applied on the titanium alloy substrate, still the percentage of dead cells did not exceed 16% and 22% for 2-day and 5-day cultures, respectively. In addition, a slight increase in cytotoxicity was observed after prolonged cell cultures of the MG-63 line.

Similarly, the TiAlV/TiO_2/hAg material showed the lowest cytotoxicity towards the HaCaT keratinocyte cells. The average percentage of live cells in direct contact with the material was over 98% after both 2 and 5 days of culture. The TiAlV/TiO_2 sample displayed the highest cytotoxicity to HaCaT cell lines after 2 and 5 days of culture, as was the case with the MG-63 cell line. Nevertheless, the average dead cell values for TiAlV/TiO_2 did not exceed 10% and 3% after 2 and 5 days of culture, respectively. The comparative analysis of the cell viability of human keratinocyte HaCaT cells after 2 and 5 days of culture revealed the decrease in cytotoxicity in direct contact with each of the tested samples along with the culture duration.

The cell viability of both the MG-63 and HaCaT lines prove that the TiAlV, TiAlV/TiO_2 and TiAlV/TiO_2/hAg samples do not show significant cytotoxic activity towards the cells tested. The obtained results prove that the prepared materials comply with the applied biocompatibility standards and can be successfully used for the veterinary treatment of long bone fractures. The viability of human osteoblastic cells (MG-63 line) was examined after direct contact with the tested TiAlV, TiAlV/TiO_2 and TiAlV/TiO_2/hAg samples to confirm the lack of cytotoxicity. The collected results are presented in Table 1 and Fig. 7A.

The analysis of the results obtained via the flow cytometry showed that the largest number of live cells (91%) was observed on the surface of the titanium alloy modified with two layers. For the TiAlV and TiAlV/TiO_2 samples, the percentage of live cells differed slightly. For the unmodified titanium alloy material, it was 82.68%, while for the titanium alloy material with TiO_2 nanotubes - 83.35%. Our in vitro experiment confirmed the lack of significant cytotoxicity of the alloys.

The images obtained from the fluorescence microscope revealed that human osteoblastic cells of the MG-63 line retained proper morphology and were evenly deposited on the substrate of TiAlV, TiAlV/TiO_2 and TiAlV/TiO_2/hAg materials (Fig. 7B). It was also noticed that the largest number of cells adhered to the outer layer containing silver nanoparticles. This phenomenon may indicate that the presence of antibacterial nanoparticles in the sol-gel layer does not affect the proper proliferation of human bone cells. Our results are consistent with other literature reports showing the positive effect of silver nanoparticles on the process of osteoblast adhesion and proliferation as well as faster regeneration of the muscle tissue [31,32]. This behavior results from the significant influence of the surface roughness on the cells adhesion. The rougher the surface is, the more willingly the cells adhere to it. It has also been proved that osteoblasts multiply much faster on substrates with different profile levels, unlike fibroblasts which prefer smooth surfaces [33].

The study also analyzed the growth of human osteoblastic cells of the MG-63 line on the TiAlV, TiAlV/TiO_2 and TiAlV/TiO_2/hAg samples using the scanning electron microscope (Fig. 7C). The pictures show regularly arranged osteoblasts on each of the surfaces. By far, the largest cells deposit was visible on the sample with two layers – a layer with TiO_2 nanotubes and a hybrid coating with antibacterial properties. In this case, osteoblasts colonized virtually the entire surface of the TiAlV/TiO_2/hAg material. Importantly, the 1000× magnification showed the areas where the cells grew in layers. In the case of the TiAlV material, osteoblasts inhabited the sample in homogeneously, which indicates their weaker adhesion to the surface layer. This phenomenon may result from the surface topography characteristics, since in the contact profilometer tests the TiAlV material had the smoothest surface of the three types of samples. According to literature reports, osteoblasts are more likely to adhere to rough substrates with differences in profile levels [34,35]. Therefore, the surface modified with the TiO_2 nanotubes layer produced by electrochemical oxidation promotes cell adhesion. Osteoblasts inhabit most of the area, in comparison with the Ti-6Al-4V titanium alloy substrate, due to the higher development of the surface layer.

The ICP-MS spectrometric analysis was performed to check the

Table 1
Flow cytometry results of percentage of live, early apoptotic, late apoptotic and dead human osteoblastic cells of the MG-63 line after a 4-day incubation with the tested materials.

MG-63 cell line (96 h)	Live Annexin V (−) 7-AAD (−)	Early apoptotic Annexin V (+) 7-AAD (−)	Late apoptotic Annexin V (+) 7-AAD (+)	Necrotic Annexin V (−) 7-AAD (+)	S/S_0/%
Control (untreated cells)	86.96	10.15	2.56	0.33	100
TiAlV	82.68	13.06	3.64	0.61	95.1
TiAlV/TiO_2	83.35	12.78	3.28	0.59	95.8
TiAlV/TiO_2/hAg	91.53	5.71	1.37	1.39	105.2

concentration of metal ions in the culture media collected after 48 and 120 h of culture and in the solutions collected after 7, 14 and 28 days of the TiAlV, TiAlV/TiO_2 and TiAlV/TiO_2/hAg samples incubation in deionized water. The obtained values of the concentrations of the analyzed ions in the tested fluids are presented in Table 2.

The obtained data have proved that the applied layers limit the release of titanium, vanadium and aluminum ions into the solution. The presence of silicon ions in the fluid is associated with the chemical composition of the synthesis precursors (TEOS and TMSPM) used during the layer production via the sol-gel method. The ICP-MS analysis confirmed that the coatings obtained through both anodization and sol-gel methods do not show significant cytotoxicity. Moreover, they constitute a barrier to the elements contained in the Ti-6Al-4V implant which could cause cytotoxic reactions if released into the surrounding tissue. As shown by recent studies [36], the vanadium concentration may contribute to the formation of allergic reactions at the biomaterial implantation site. In our work, the vanadium concentration amounted to less than 0.001 ppm after 7, 14 and 28 days of the samples incubation in deionized water.

The antimicrobial activity of silver nanoparticles depends mainly on the amount of released ions. Ag + ions are released when they come into contact with the aquatic environment [37]. Ziabka et al. [32,38] in her earlier proved that the Ag + release depended on the immersion time, increasing as a function of time, yet the highest increase was observed during the first month of the sample incubation.

For the TiAlV/TiO_2/hAg sample, the ICP-MS analysis showed that the release of silver ions depended primarily on the incubation time in deionized water. The Ag + ions concentration increases as a function of time, although the largest increase occurred at the first stage of the experiment - after 7 days of the sample incubation. Although the content of silver ions in the tested solution is insignificant, not exceeding 8.0 ppm, it is sufficient for a satisfactory bactericidal effect. The evaluated antibacterial activity of the TiAlV/TiO_2/hAg sample against the standard bacterial strains: *Escherichia coli* and *Staphylococcus aureus* confirmed this effect. The conducted assessment showed the complete inhibition of the bacteria growth (Table 3). On the other hand, the tests did not show bactericidal effectiveness for the Ti-6Al-4V titanium alloy material and for the samples coated with the TiO_2 nanotubes layer. The obtained results confirmed the effective bactericidal effect only of the hybrid coating containing silver nanoparticles which are necessary to eliminate Gram-negative and Gram-positive bacteria. The obtained results stay in line with the previous literature reports [39,40].

Due to the effective activity against fungus and bacteria, the novel materials enriched with noble metal ions, such as silver, cobalt or copper, offer a promising prospect for the development of medical devices. Today a range of products chemically active against microorganisms is limited to medical bandages and sportswear to avoid infections and odors [41]. The sol-gel technology allows one to produce hybrid materials enhanced with different components, such as inorganic salts or organic additives. Therefore, it is possible to develop functional materials for different purposes [42]. In our previous work we proved that the proper concentration of silver may act as a bactericidal agent without cytotoxic effect [38] and the nanotubular structure may increase the cells viability [43].

3. Conclusions

In this work we developed the medical implants intended for long bone anastomoses in animals and evaluated their physicochemical and biological properties. The composite plates made of the Ti-6Al-4V titanium alloy were covered with two layers. The inner layer of TiO_2 titanium dioxide nanotubes was obtained via the electrochemical oxidation, while the external hybrid coating with bactericidal properties was prepared using the sol-gel method. A set of examinations was performed to assess the surface properties, microstructural analysis and phase composition, as well as biological properties of the implants. Based on the conducted research, it was found that the TiO_2 nanotube layer on the Ti-6Al-4V titanium alloy increased the surface development. The substrate changed its nature from hydrophilic to hydrophobic, thus protecting the implants against corrosion and scratches. The silver nanoparticles dispersed in the outer coating increased the surface roughness. The biological studies proved that human bone cells were more prone to adhesion and proliferation on the surfaces with differentiated profile levels. The cytotoxicity tests consisted in the direct in vitro contact of the TiAlV alloy and its modifications with the two human cell lines: the osteoblast-like MG-63 and the keratinocyte HaCaT. The observations after 72 h showed no significant changes in the cell morphology and viability in the case of all the samples. The microstructural tests confirmed that the electrochemical oxidation and the sol-gel methods were effective ways to produce layers on elements of complex shapes, such as bone anastomosis plates. The ICP-MS research revealed that the coatings prevented the penetration of disadvantageous elements, e.g. vanadium, from the sample substrate into the surrounding environment. It was also proved that the hybrid layers were biocompatible and did not show cytotoxic activity. Therefore, it can be presumed that the tested materials will be characterized by good biocompatibility in vivo. Moreover, the silver nanoparticles from the outer layer of the implant exhibit antibacterial activity of Gram-negative (*Escherichia coli*) and Gram-positive (*Staphylococcus aureus*) bacteria, which is a beneficial phenomenon in the bone tissue treatment.

4. Materials and methods

4.1. Material manufacturing

Sterile metallic implants (straight compression plates for 2.0 system, 14 hole) for osteosynthesis of long bones in animals made of the TiAlV alloy were manufactured by Medgal (Księżno, Poland) and delivered by the “Pulawska” veterinary clinic (Warsaw, Poland). Antibacterial hybrid coatings were applied to their surface by two methods: the electrochemical oxidation (anodization) and the sol-gel method. Prior to the anodization process, the plates were degresed with an ultrasonic washer, the implants were rinsed in acetone, isopropanol and then in distilled water. Each rinse cycle lasted 10 min. Then the plates were allowed to air dry. The TiO_2 nanotubes were obtained in a two-electrode system where the titanium alloy plate played the role of an anode, while the platinum electrode (the platinum plate coated with platinum black) was the cathode. The anodization process lasted for 2 h at the 30 V voltage in an electrolyte consisting of a glycerin solution with the

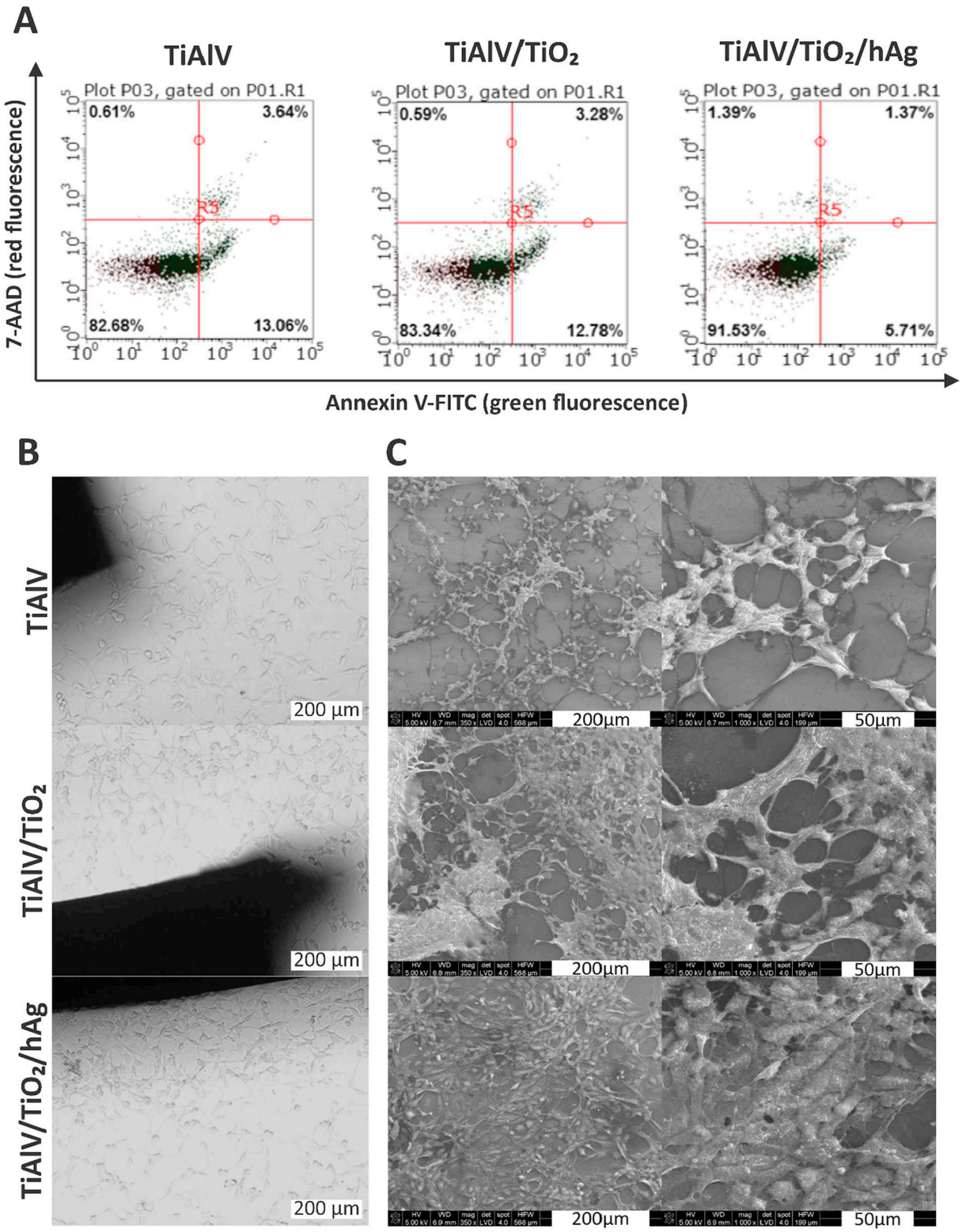

Fig. 7. Cytogram showing the percentage of live, early apoptotic, late apoptotic and dead human osteoblastic cells of the MG-63 line after a 4-day incubation with the tested materials (A); Optical microscope images (B) and SEM (C) micrographs of human osteoblastic cells of the MG-63 line after a 4-day incubation with the tested materials.

addition of 23% distilled water and 0.25% ammonium fluoride, according to the method described in papers of Kusior et al. and Radecka et al. [44,45]. The samples with the applied layer were cleaned in an ultrasonic scrubber and annealed in argon flow to increase the crystallinity of the produced coating.

The second layer was an organic-inorganic silicate coating modified with silver compounds. The coating solution was prepared via the sol-gel method, using the following TEOS precursors: (tetrethylorthosilicate, Si (OC_2H_5) 4) 40 mol% - TMSPM (3-(Trimethoxysilyl) propyl methacrylate, H_2C = C (CH_3) CO_2 (CH_2) 3Si

Table 2
ICP-MS analysis of the culture media after 48 h and 120 h incubation of samples, the solutions after 7, 14 and 28 days of samples incubation in deionized water.

MG-63 cell line	Metal ions content [ppm]				
	Al	Si	Ti	V	Ag
48 h					
Control (untreated cells)	0.002	0.317	< 0.002	0.007	< 0.001
TiAlV	< 0.001	0.342	< 0.002	0.008	< 0.001
TiAlV/TiO_2	< 0.001	0.318	< 0.002	0.009	< 0.001
TiAlV/TiO_2/hAg	< 0.001	0.779	< 0.002	0.009	< 0.001
120 h					
Control (untreated cells)	< 0.001	0.288	< 0.002	0.008	< 0.001
TiAlV	< 0.001	0.367	< 0.002	0.010	< 0.001
TiAlV/TiO_2	< 0.001	0.403	< 0.002	0.012	< 0.001
TiAlV/TiO_2/hAg	< 0.001	0.654	< 0.002	0.011	< 0.001
UHQ	7 days				
TiAlV	< 0.001	< 0.001	< 0.002	< 0.001	< 0.002
TiAlV/TiO_2	< 0.001	< 0.001	< 0.002	< 0.001	< 0.002
TiAlV/TiO_2/hAg	< 0.001	< 0.001	< 0.002	< 0.001	5.137
UHQ	14 days				
TiAlV	0.008	0.014	< 0.002	< 0.001	0.008
TiAlV/TiO_2	0.002	0.006	< 0.002	< 0.001	0.012
TiAlV/TiO_2/hAg	0.013	0.319	< 0.002	< 0.001	8.284
UHQ	28 days				
TiAlV	0.023	0.039	< 0.002	< 0.001	< 0.002
TiAlV/TiO_2	0.011	0.014	< 0.002	< 0.001	< 0.002
TiAlV/TiO_2/hAg	0.040	2.508	0.005	< 0.001	8.716

Table 3
Bactericidal effect of the TiAlV, TiAlV/$TiO_2$and TiAlV/TiO_2/hAg samples.

Bacteria type	*Escherichia coli* ATTC 25922	Staphylococcus aureus ATTC 25923
Material	Colony forming unit/1 mL	
Control	9×10^4	5×10^4
TiAlV	1.5×10^4	1.7×10^4
TiAlV/TiO_2	1.1×10^5	1.1×10^4
TiAlV/TiO_2/hAg	0	0

(OCH_3) 3) 50 mol% - TIP (titanium (IV) isopropoxideTi (OC_3H_7) 4) 5 mol% - $AgNO_3$ 5 mol%. First, silver nitrate was dissolved in propanol serving as a solvent. The solution mixed for 30 min in a magnetic stirrer. Next, TEOS, TMSPM and TIP were successively added to the solution. Having introduced each of the reagents, the solution was stirred for another 20 min. The aqueous solution of HNO_3 nitric acid was used as a reaction catalyst. The volume ratio of all the components to the propanol solvent was 1: 8. Prior to layering, the solution aging time was 24 h and the viscosity equaled 6 cP. The obtained sol was stored in a sealed container, with no access to UV and VIS radiation in order to limit Ag + reduction. The plates were washed with propyl alcohol. The layers were applied by immersion and then the plates were drying in ambient conditions for 24 h. Then, the applied layers underwent the thermal curing process at 80 °C for 10 min and 130 °C for 15 min.

The following nomenclature was adopted to standardize the names of the samples in this work (Table 4). The bone anastomosis plates which were covered with the antibacterial hybrid coatings are shown in Fig. 8.

Table 4
Samples nomenclature.

Sample characteristic	Sample nomenclature
Titanium alloy Ti-6Al-4V	TiAlV
Titanium alloy Ti-6Al-4V with TiO_2 nanotube layer	TiAlV/TiO_2
Titanium alloy Ti-6Al-4V with TiO_2 nanotube layer and hybrid layer containing silver nanoparticles AgNPs	TiAlV/TiO_2/hAg

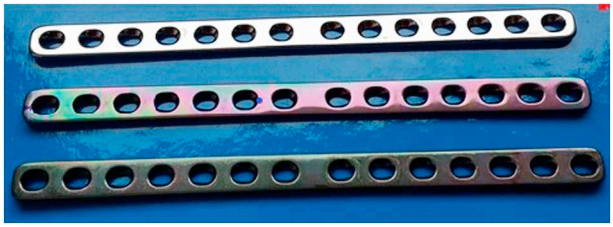

Fig. 8. Plates made of titanium alloy (Ti-6Al-4V) for osteosynthesis in animals. From the top: TiAlV plate, TiAlV/TiO_2 plate and TiAlV/TiO_2/hAg plate.

4.2. Material evaluation, scanning electron microscopy

The detailed microstructure examination of the materials was carried out by means of the Nova NanoSEM 200 scanning electron microscope (FEI, Eindhoven, The Netherlands) with the Genesis XM X-ray microanalysis system (EDAX, Tilburg, The Netherlands) featuring the EDAX Sapphire Si(Li) EDX detector. The observations and measurements took place in low vacuum conditions, using Helix detector (SE) with the accelerated voltage of 10–18 kV.

4.3. Roughness

The arithmetical mean roughness (*Ra*) and the root mean square roughness (*Rq*) of investigated materials were evaluated by means of the contact profilometer HOMMEL-ETAMIC T1000 wave (Jenoptik AG, Jena, Germany). The arithmetical mean roughness values were an average of 10 measurements expressed as the mean ± standard deviation (SD).

4.4. Atomic force microscopy

The topography imaging was performed using MultiMode VIII (Bruker, Karlsruhe, Germany) atomic force microscope working in the contact mode in air. The silicon nitride tips with 2 nm nominal radius and cantilevers with 0.175 N/m nominal spring constant were used. The arithmetical mean roughness (*Ra*) and root mean square roughness (*Rq*) were calculated from ten 2 μm × 2 μm areas.

4.5. Surface wettability

The static water contact angle was used to assess the surface wettability via the sessile drop method with the automatic drop shape analysis system DSA 10 Mk2 (Kruss GmbH, Hamburg, Germany). The constant temperature and humidity conditions were maintained throughout the tests while the UHQ-water droplets of 0.25 μL were applied on each pure and dry sample. We calculated the apparent contact angle as an average of 30 measurements and expressed it as the mean ± standard deviation (SD).

4.6. Free surface energy

The free surface energy was determined by testing the contact angles of two measuring liquids - ultra pure distilled water (UHQ PURE Lab, Vivendi Water) and diiodomethane. The measurements were carried out on the DSA 10 Mk2 optical apparatus (Kruss GmbH, Hamburg, Germany) at room temperature. The test pattern was identical to the contact angle test. The obtained photos of drops of two measuring liquids established the free surface energy based on the values of the dispersion and polar components. The value is the arithmetic average obtained from 30 measurements. The results are presented with standard deviations (SD).

4.7. XRD X-ray diffractometry

The phase composition of the materials was determined using the PANalytical X-ray diffractometer, Empyrean model. The measurements were taken using the monochrome radiation with the wavelength corresponding to the emission line (Cu Kα1). The diffractograms were recorded in the 2θ angle range = 5–90°, and the goniometer step was 0.008°. The qualitative analysis of the phase composition was made using the X'PertHighScore Plus computer program developed by PANalytical.

4.8. Cell cultures

The human osteoblast-like MG-63 cell line (ATCC: CRL-1427™) and the human keratinocyte HaCaT cell line (CSL Cell Lines Service GmbH) were cultured in Dulbecco's Modified Eagle's Medium (DMEM, Corning) with phenol red, supplemented with 10% heat-inactivated fetal bovine serum (FBS) and with 1% streptomycin/penicillin. The cells were incubated at 37 °C in the humidified atmosphere containing 5% CO_2. The cells were cultured to the confluence of the culture plate and the passages were performed at least twice a week, using the solution containing 0.05% trypsin and 0.5 mM EDTA. All the media and other ingredients were purchased from ALAB (Warsaw, Poland).

4.9. Cytotoxic study in vitro

The cytotoxicity was examined according to the ISO 10993-5 norm "Biological evaluation of medical devices – Test for cytotoxicity: *in vitro* methods" [46]. The TiAlV, TiAlV/TiO_2, and TiAlV/TiO_2/hAg alloys were tested in vitro as the rectangular/quadrate/round samples (width / length / height − 3.5 × 7.9 × 2.0 mm). Prior to the treatment, the alloys were sterilized using the steam sterilizer (NÜVE) for 20 min at 132 °C. It was proved that the sterilization process did not change the structure/morphology of the resulting coatings (data shown in the supplementary file, Fig. S1). The alloys were placed in the appropriate polystyrene culture plates (NEST) and the cell suspension was poured over the surface of the tested samples. The plates were incubated in the dark in the standard cell conditions (37 °C, 5% CO_2) for a designed period of time.

The cytotoxic activity of TiAlV, TiAlV/TiO_2, and TiAlV/TiO_2/hAg towards the MG-63 and HaCaT cell lines was examined using the Alamar Blue assay after direct contact treatment. The cell viability was evaluated according to the modified protocol provided by the manufacturer (Alamar Blue™ Cell Viability Assay, Thermo SCIENTIFIC). In brief, the 2×10^4/2 mL cells per well, seeded in a 12-well flat bottom microtiter plate, were incubated with the tested alloys for 48, 72 and 96 h. Every 24 h the cells were washed three times with the phosphate-buffered saline (PBS: NaCl, KCl, Na_2HPO_4, KH_2PO_4, pH = 7.4) and the fresh medium was applied. In each case, the post-incubation medium was collected and the ICP-MS analysis was carried out to determine the concentration of the released metal ions (vide infra). To assess the cell viability at each time point of the experiment the cells were washed with PBS and incubated with the resazurin sodium salt solution (25 mM in PBS) for 3 h in the dark at 37 °C. The fluorescence caused by the cellular metabolic activity was measured at 605 nm (excitation wavelength 560 nm) with the multimode microplate reader (Infinite 200 M PRO NanoQuant, Tecan, Männedorf, Switzerland). The cytotoxicity was expressed as the percentage of viable cells after the treatment with the tested alloys in reference to the untreated cells (the control). The experiment was repeated at least three times and the determined values of surviving fraction (S/So, %) are expressed as the mean + S.D. (Standard Deviation).

4.10. Cell viability assessed by flow cytometry

The cell viability after the treatment with studied alloys was assessed by means of the flow cytometry. The Annexin V Apoptosis Detection Kit FITC (Invitrogen) and the eBioscience™ 7-AAD Viability Staining Solution (ThermoFischer SCIENTIFIC) were used to quantitatively detect apoptotic and necrotic cells, respectively. The 2×10^5/2 mL MG-63 and HaCat cells were incubated with the TiAlV, TiAlV/TiO_2, and TiAlV/TiO_2/hAg samples in 6-well plates for 96 h in the standard culture conditions. Every 24 h the medium was exchanged for the new one. After 96 h, the cells were washed twice with the PBS buffer and trypsinized. Then, the cells were collected and centrifuged. The cells separated from the supernatant were washed twice with the 0.5 mL PBS buffer and suspended in the Binding Buffer. Fifteen minutes before the measuring procedure, the cells were stained with the Annexin V-FITC and 7-AAD while incubated in the dark. The viable and dead (early apoptotic, late apoptotic, and necrotic) cells were detected and counted with the application of Guava® easyCyte™, Germany. The experiment was repeated two times.

4.11. Microscopic visualization

The cells morphology during the treatment with the studied alloys was monitored using the fluorescence inverted microscope (Olympus IX51, Tokio, Japan). The photographs of the cells during the treatment in the transmitted light mode were taken under the 20× magnification.

4.12. Analysis of cell growth by SEM

To conduct the SEM analysis, the cells with the tested materials were incubated for 96 h in the standard conditions (37 °C, 5% CO_2). Then, the plates were washed carefully with PBS, fixed overnight in the 4% glutaraldehyde solution at 4 °C and dehydrated in graded alcohol ranging from 10% to 100% ethanol for 10 min each. The samples were examined with the scanning electron microscope Nova NanoSem 200 (FEI Company, Eindhoven, the Netherlands) using the low vacuum detector (LVD) at the 5 kV accelerating voltage at various magnifications.

4.13. Release of metal ions analyzed by ICP-MS

The TiAlV, TiAlV/TiO_2 and TiAlV/TiO_2/hAg implants were incubated in tightly closed, sterile polypropylene containers placed in 30 mL of ultrahigh quality deionized water (diUHQ) at 37 °C ± 1 °C for one month. The sample weight to incubation medium ratio equaled 1 g:10 mL, which complied with the ISO 10993-15:2019 standard "Part 15: Identification and quantification of degradation products from metals and alloys" [47]. The examinations were performed after 7, 14 and 28 days of incubation.

The in vitro release of metal ions was studied by means of the Inductively Coupled Plasma Mass Spectrometry (ICP-MS), using the ICP-MS Perkin-Elmer Plasma 6100 spectrometer. Prior to the tests, the filtered samples were acidified with nitric acid up to the final concentration of 0.1 mol/L in order to prohibit the silver ions (Ag+) reduction into metallic silver. The silver concentration values were determined using the ICP-MS at *m/z* 107, applying the external standard calibration procedure. After each experiment, the cell culture medium was collected after 48 and 120 h and analyzed in terms of the Ti, V, Si Al, and Ag ions content.

4.14. In vitro bactericidal efficacy tests

The TiAlV, TiAlV/TiO_2 and TiAlV/TiO_2/hAg samples (4 of each group) were tested to establish the bactericidal efficacy, using the modified method according to the ASTM E 2180–07 norm "Standard Test Method for Determining the Activity of Incorporated Antimicrobial Agent(s) In Polymeric or Hydrophobic Materials" [48]. The only alteration was introduced to match the norm to the metallic samples size. Each sample was tested according to the following procedure. First, the

bacterial suspensions ($1.5 * 10^5$ CFU/mL) [CFU – *colony forming unit* – a measure of viable bacterial cells] were prepared for *Staphylococcus aureus* ATCC 19660 and *Escherichia coli* ATTC 25922. Next, the solution consisting of 0.3% agar solution and 0.85% NaCl (soft-top agar) solution was prepared. Then 1 mL of bacterial suspension (separately for each bacterial species) was added to 100 mL of soft-top agar. The three manufactured samples were incubated in DMEM (ATCC, USA) containing 10% FBS (HyClone, USA) for 7 days and then placed in 6-well cell culture plates (wells of 3.5 cm in diameter). One type of bacteria was applied into one well. The samples did not come in any physical contact in the course of the experiment. 50 μL of the soft-top agar bacterial suspension was placed on the samples that were incubated for 24 h at 37 °C. After 24 h, the polymer samples were transferred to 5 mL-test tubes containing 2 mL of BHI broth (Brain Heart Infusion). The test tubes were treated with ultrasounds for 1 min at room temperature and vortexed (0.5 h) to transfer bacteria to the medium. At the next stage 400 μL of the BHI-bacteria suspension was mixed with 600 μL of straight BHI. Subsequently, 100 μL was planted on the BHI agar medium composition and incubated for 24 h at 37 °C. After the incubation the bacteria colonies were counted.

4.15. Statistical analysis

The results were analyzed using one-way analysis of variance (ANOVA) with Duncan post-hoc tests, which were performed with Statistica 13.1 software (TIBCO Software Inc., Palo Alto, California, USA). The results were considered statistically significant when $p < 0.05$.

Supplementary data to this article can be found online at https://doi.org/10.1016/j.msec.2020.110968.

Funding

This work was carried out within statutory research realized at the Faculty of Materials Science and Ceramics AGH University of Science and Technology, No. 11.11.160.557.

CRediT authorship contribution statement

Magdalena Ziąbka: Conceptualization, Validation, Formal analysis, Data curation, Writing - original draft, Writing - review & editing. **Joanna Kiszka**: Formal analysis, Writing - review & editing. **Anita Trenczek-Zając**: Resources. **Marta Radecka**: Resources. **Katarzyna Cholewa-Kowalska**: Resources. **Igor Bissenik**: Resources. **Agnieszka Kyzioł**: Investigation, Formal analysis. **Michał Dziadek**: Visualization. **Wiktor Niemiec**: Formal analysis. **Aleksandra Królicka**: Formal analysis.

Declaration of competing interest

The authors declare that they have no known competing financial interests or personal relationships that could have appeared to influence the work reported in this paper.

Acknowledgements

The authors would like to thank Janusz M. Dabrowski for the access to the cytometer Guava® easyCyteTM.

References

[1] U. Matis, Current techniques of fracture fixation in dogs and cats, World Small Animal Veterinary Association World Congress Proceedings, 2007.
[2] A.L. Johnson, J.E.F. Houlton, R. Vannini, Fractures of the proximal tibia, AO Principles of Fracture Management in the Dog and Cat, AO Publishing, Switzerland, 2005.
[3] D. Hulse, K. Ferry, A. Fawcett, D. Gentry, W. Hyman, S. Geller, M. S, Effect of intramedullary pin size on reducing bone plate strain, Vet. Comp. Orthop. Traumatol. 13 (2000) 185–190.
[4] K.M. Tobias, S.A. Johnston, Fractures of the tibia and fibula, Veterinary Surgery Small Animal, Elsevier Health Sciences, 2013.
[5] M. Geetha, A.K. Singh, R. Asokamani, A.K. Gogia, Ti based biomaterials, the ultimate choice for orthopaedic implants - a review, Prog. Mater. Sci. 54 (3) (2009) 397–425, https://doi.org/10.1016/j.pmatsci.2008.06.004.
[6] S. Ferraris, S. Spriano, Antibacterial titanium surfaces for medical implants, Mater. Sci. Eng. C 61 (2016) 965–978, https://doi.org/10.1016/j.msec.2015.12.062.
[7] Z. Jia, P. Xiu, P. Xiong, W. Zhou, Y. Cheng, S. Wei, Y. Zheng, T. Xi, H. Cai, Z. Liu, et al., Additively manufactured macroporous titanium with silver-releasing micro-/Nanoporous surface for multipurpose infection control and bone repair - a proof of concept, ACS Appl. Mater. Interfaces 8 (42) (2016) 28495–28510, https://doi.org/10.1021/acsami.6b10473.
[8] X. Liu, H.C. Man, Laser fabrication of Ag-HA nanocomposites on Ti6Al4V implant for enhancing bioactivity and antibacterial capability, Mater. Sci. Eng. C 70 (2017) 1–8, https://doi.org/10.1016/j.msec.2016.08.059.
[9] T. Zhou, Y. Zhu, X. Li, X. Liu, K.W.K. Yeung, S. Wu, X. Wang, Z. Cui, X. Yang, P.K. Chu, Surface functionalization of biomaterials by radical polymerization, Prog. Mater. Sci. 83 (2016) 191–235, https://doi.org/10.1016/j.pmatsci.2016.04.005.
[10] Y. Zhang, C. Dong, S. Yang, J. Wu, K. Xiao, Y. Huang, X. Li, Alkalescent nanotube films on a titanium-based implant: a novel approach to enhance biocompatibility, Mater. Sci. Eng. C 72 (2017) 464–471, https://doi.org/10.1016/j.msec.2016.11.096.
[11] M. Li, X. Liu, Z. Xu, K.W.K. Yeung, S. Wu, Dopamine modified organic-inorganic hybrid coating for antimicrobial and osteogenesis, ACS Appl. Mater. Interfaces 8 (49) (2016) 33972–33981, https://doi.org/10.1021/acsami.6b09457.
[12] J.A. Disegi, L. Eschbach, Stainless steel in bone surgery, Injury 31 (Suppl. 4) (2000) 2–6, https://doi.org/10.1016/S0020-1383(00)80015-7.
[13] S. Faegh, H.-Y. Chou, S. Muftu, Load transfer along the bone-implant Interface and its effects on bone maintenance, Implant Dentistry - a Rapidly Evolving Practice, InTech, 2011, , https://doi.org/10.5772/18433.
[14] L.C. Vaughan, Complications associated with the internal fixation of fractures in dogs, J. Small Anim. Pract. 16 (1 − 12) (1975) 415–426, https://doi.org/10.1111/j.1748-5827.1975.tb05765.x.
[15] B.S. Smith, S. Yoriya, T. Johnson, K.C. Popat, Dermal fibroblast and epidermal keratinocyte functionality on titania nanotube arrays, Acta Biomater. 7 (6) (2011) 2686–2696, https://doi.org/10.1016/j.actbio.2011.03.014.
[16] K. Gulati, M.S. Aw, D. Losic, Drug-eluting Ti wires with titania nanotube arrays for bone fixation and reduced bone infection, Nanoscale Res. Lett. 6 (1) (2011) 1–6, https://doi.org/10.1186/1556-276X-6-571.
[17] A. Kodama, S. Bauer, A. Komatsu, H. Asoh, S. Ono, P. Schmuki, Bioactivation of titanium surfaces using coatings of TiO_2 nanotubes rapidly pre-loaded with synthetic hydroxyapatite, Acta Biomater. 5 (6) (2009) 2322–2330, https://doi.org/10.1016/j.actbio.2009.02.032.
[18] B.S. Smith, S. Yoriya, L. Grissom, C.A. Grimes, K.C. Popat, Hemocompatibility of titania nanotube arrays, J. Biomed. Mater. Res. - Part A 95 A (2) (2010) 350–360, https://doi.org/10.1002/jbm.a.32853.
[19] K.S. Brammer, S. Oh, C.J. Cobb, L.M. Bjursten, H. van der Heyde, S. Jin, Improved bone-forming functionality on diameter-controlled TiO_2 nanotube surface, Acta Biomater. 5 (8) (2009) 3215–3223, https://doi.org/10.1016/j.actbio.2009.05.008.
[20] S. Yeniyol, Z. He, B. Yüksel, R.J. Boylan, M. Ürgen, T. Özdemir, J.L. Ricci, Antibacterial activity of as-annealed TiO_2 nanotubes doped with Ag nanoparticles against periodontal pathogens, Bioinorg. Chem. Appl. 2014 (2014), https://doi.org/10.1155/2014/829496.
[21] S.M. Lee, B.S. Lee, T.G. Byun, K.C. Song, Preparation and antibacterial activity of silver-doped organic-inorganic hybrid coatings on glass substrates, Colloids Surfaces A Physicochem. Eng. Asp. 355 (1–3) (2010) 167–171, https://doi.org/10.1016/j.colsurfa.2009.12.010.
[22] R.A. Procaccini, C.A. Studdert, S.A. Pellice, Silver doped silica-methyl hybrid coatings. Structural evolution and antibacterial properties, Surf. Coatings Technol. 244 (2014) 92–97, https://doi.org/10.1016/j.surfcoat.2014.01.036.
[23] P. Exnar, I. Iovětinská-Slamborová, I.D. Veverková, Antimicrobial hybrid nano-layers prepared by sol-gel method, NanoCon; Brno, 2015.
[24] L. Zhao, L. Liu, Z. Wu, Y. Zhang, P.K. Chu, Effects of micropitted/nanotubular titania topographies on bone mesenchymal stem cell osteogenic differentiation, Biomaterials 33 (9) (2012) 2629–2641, https://doi.org/10.1016/j.biomaterials.2011.12.024.
[25] N. Wang, H. Li, W. Lü, J. Li, J. Wang, Z. Zhang, Y. Liu, Effects of TiO_2 nanotubes with different diameters on gene expression and osseointegration of implants in minipigs, Biomaterials 32 (29) (2011) 6900–6911, https://doi.org/10.1016/j.biomaterials.2011.06.023.
[26] L. Zhao, H. Wang, K. Huo, L. Cui, W. Zhang, H. Ni, Y. Zhang, Z. Wu, P.K. Chu, Antibacterial nano-structured titania coating incorporated with silver nanoparticles, Biomaterials 32 (24) (2011) 5706–5716, https://doi.org/10.1016/j.biomaterials.2011.04.040.
[27] P.I. Brånemark, B.O. Hansson, R. Adell, U. Breine, J. Lindström, O. Hallén, A. Ohman, Osseointegrated implants in the treatment of the edentulous jaw. experience from a 10-year period, Scand. J. Plast. Reconstr. Surg. Suppl. 16 (1977) 1–132.
[28] K. Huo, X. Zhang, H. Wang, L. Zhao, X. Liu, P.K. Chu, Osteogenic activity and antibacterial effects on titanium surfaces modified with Zn-incorporated nanotube arrays, Biomaterials 34 (13) (2013) 3467–3478, https://doi.org/10.1016/j.biomaterials.2013.01.071.
[29] A. Iglic, Gongadze, D. Kabaso, Bauer, P. Schmuki, Slivnik, U. van Rienen, Adhesion

of osteoblasts to a nanorough titanium implant surface, Int. J. Nanomedicine 6 (2011) 1801, https://doi.org/10.2147/ijn.s21755.
[30] K.J. Kubiak, M.C.T. Wilson, T.G. Mathia, P. Carval, Wettability versus roughness of engineering surfaces, Wear 271 (3–4) (2011) 523–528, https://doi.org/10.1016/j.wear.2010.03.029.
[31] M. Ziąbka, A. Mertas, W. Król, J. Chłopek, Preliminary biological evaluation of polyoxymethylene/nanosilver composites, Eng. Biomater. 12 (2009) 89–91.
[32] M. Ziabka, E. Menaszek, J. Tarasiuk, S. Wroński, Biocompatible nanocomposite implant with silver nanoparticles for otology—in vivo evaluation, Nanomaterials 8 (10) (2018), https://doi.org/10.3390/nano8100764.
[33] H. Özçelik, C. Padeste, V. Hasirci, Systematically organized nanopillar arrays reveal differences in adhesion and alignment properties of BMSC and Saos-2 cells, Colloids Surfaces B Biointerfaces 119 (2014) 71–81, https://doi.org/10.1016/j.colsurfb.2014.03.019.
[34] D. Yamashita, M. Machigashira, M. Miyamoto, H. Takeuchi, K. Noguchi, Y. Izumi, S. Ban, Effect of surface roughness on initial responses of osteoblast-like cells on two types of zirconia, Dent. Mater. J. 28 (4) (2009) 461–470, https://doi.org/10.4012/dmj.28.461.
[35] M.F. Solá-Ruiz, C. Pérez-Martínez, J.J. Martín-del-Llano, C. Carda-Batalla, C. Labaig-Rueda, In vitro preliminary study of osteoblast response to surface roughness of titanium discs and topical application of melatonin, Med. Oral Patol. Oral Cir. Bucal. 20 (1) (2015) e88–e93, https://doi.org/10.4317/medoral.19953.
[36] S.D. Rogers, D.W. Howie, S.E. Graves, M.J. Pearcy, D.R. Haynes, In vitro human monocyte response to wear particles of titanium alloy containing vanadium or niobium, J. Bone Joint Surg. Br. 79-B (2) (1997) 311–315, https://doi.org/10.1302/0301-620x.79b2.0790311.
[37] D. Patil, M.K. Wasson, S. Aravindan, P. Vivekanandan, P.V. Rao, Antibacterial and cytocompatibility study of modified Ti6Al4V surfaces through thermal annealing, Mater. Sci. Eng. C 99 (2019) 1007–1020, https://doi.org/10.1016/j.msec.2019.02.058.
[38] M. Ziąbka, M. Dziadek, E. Menaszek, R. Banasiuk, A. Królicka, Middle ear prosthesis with bactericidal efficacy-in vitro investigation, Molecules 22 (10) (2017), https://doi.org/10.3390/molecules22101681.
[39] D.S.W. Benoit, K.R. Sims, D. Fraser, Nanoparticles for oral biofilm treatments, ACS Nano 13 (5) (2019) 4869–4875, https://doi.org/10.1021/acsnano.9b02816.
[40] M. Ziabka, M. Dziadek, A. Królicka, Biological and physicochemical assessment of middle ear prosthesis, Polymers (Basel) 11 (1) (2019), https://doi.org/10.3390/polym11010079.
[41] R. Procaccini, A. Bouchet, J.I. Pastore, C. Studdert, S. Ceré, S. Pellice, Silver-functionalized methyl-silica hybrid materials as antibacterial coatings on surgical-grade stainless steel, Prog. Org. Coatings 97 (2016) 28–36, https://doi.org/10.1016/j.porgcoat.2016.03.012.
[42] I. Šlamborová, V. Zajícová, J. Karpíšková, P. Exnar, I. Stibor, New type of protective hybrid and nanocomposite hybrid coatings containing silver and copper with an excellent antibacterial effect especially against MRSA, Mater. Sci. Eng. C 33 (1) (2013) 265–273, https://doi.org/10.1016/j.msec.2012.08.039.
[43] A. Fraczek-Szczypta, E. Menaszek, S. Blazewicz, Influence of different types of carbon nanotubes on muscle cell response, Mater. Sci. Eng. C 46 (2015) 218–225, https://doi.org/10.1016/j.msec.2014.10.036.
[44] A. Kusior, A. Wnuk, A. Trenczek-Zajac, K. Zakrzewska, M. Radecka, TiO_2 nanostructures for photoelectrochemical cells (PECs), Int. J. Hydrog. Energy 40 (14) (2015) 4936–4944, https://doi.org/10.1016/j.ijhydene.2015.01.103.
[45] M. Radecka, A. Wnuk, A. Trenczek-Zajac, K. Schneider, K. Zakrzewska, TiO_2/SnO_2 nanotubes for hydrogen generation by photoelectrochemical water splitting, Int. J. Hydrog. Energy 40 (1) (2015) 841–851, https://doi.org/10.1016/j.ijhydene.2014.09.154.
[46] ISO - ISO 10993-5, Biological evaluation of medical devices — part 5: tests for in vitro cytotoxicity, https://www.iso.org/standard/36406.html, (2009) , Accessed date: 26 February 2020.
[47] ISO - ISO 10993-15, Biological Evaluation of Medical Devices — Part 15: Identification and Quantification of Degradation Products From Metals and Alloys, https://www.iso.org/standard/68937.html, (2019) , Accessed date: 26 February 2020.
[48] ASTM E2180, 18 Standard Test Method for Determining the Activity of Incorporated Antimicrobial Agent(S) in Polymeric or Hydrophobic Materials, https://www.astm.org/Standards/E2180 , Accessed date: 26 February 2020.